

2004 Annual Report Conference on Electrical Insulation and Dielectric Phenomena  
**Numerical simulation and optimization of electrostatic air pumps**

N. E. Jewell-Larsen, D. A. Parker, I. A. Krichtafovitch\*, and A. V. Mamishev

\*Kronos Air Technologies, Redmond, WA 98052, USA

Sensors, Energy, and Automation Lab (SEAL), University of Washington, Seattle, WA 98105, USA

**Abstract:** Electrostatic air propulsion is a promising technology with such potential applications as energy-efficient ventilation, cooling of electronics, and dehumidification. The challenges of existing designs include the need to increase air speed, backpressure, energy efficiency, heat exchange capability, and longevity. This paper presents the numerical simulation results of an electrostatic air pump for the purpose of optimizing device characteristics through control of the inner pump electric field profile. A sharp-edge-to-parallel-plane electrode geometry with unipolar positive corona is chosen to generate linear electric field distribution and minimize energy loss. Simulations were performed for multiple collector electrode voltage distributions. A method to quantify the change in pump performance between different voltage distributions is presented. The influence of space charge on pump performance is also discussed. The ultimate goal is to create multi-channel energy efficient ionic pumps, however, single cell analysis is conducted in this study as a building block of future designs.

**Introduction**

Electrostatic air pumps, also known as ionic wind pumps, have been examined as an alternative to rotary fans in such applications as air propulsion and cooling, [1,2]. They are also being studied for such applications as bacteria control and dehumidification. The classical rotary structural geometry, although used in numerous applications, is limited in both scale and design due to the necessity of high-speed rotating parts. Turbulent flow, vibration, and gyroscopic forces introduce inherent inefficiency and noise to a rotary system. Even in the applications when noise and vibrations do not present a significant problem, rotary fans are difficult to optimize for more than a single air flow circulation pattern, due to their nearly static cross-sectional air velocity profile. Ionic wind pumps offer nearly laminar air propulsion with dynamic airflow profiles, controllable air velocities, and, in some designs, a decrease in the boundary layer at the solid-fluid interface [3]. In addition, ionic propulsion is achieved without moving mechanical parts, thus enabling flexible design and possible integration on the MEMS level [4,5]. Existing electrostatic air propulsion devices have simple electrode geometry, which is convenient for theoretical modeling but sub-optimal in terms of air speed, backpressure, efficiency, and longevity. Significant room for corona technology evolution exists on the path towards practical devices and applications.

Earlier studies of ionic wind pump optimization concentrated on geometric modifications of device design by investigating the effect of collector electrode orientation with respect to the corona electrode and its

influence on field line geometry and air flow efficiency [2]. The influence of geometry and distributed voltage on pump performance was investigated in [6]. Although that study demonstrated enhanced pump performance, it lacked exploration into optimal electric field distributions. Further advancements in pump performance require taking into consideration the effects of space charge and collector surface voltage distributions in order to find optimum device parameters and performance. The influence of collector surface voltage and space charge are studied using finite element simulations.

The mechanism of corona-induced ionic wind propulsion is illustrated in Figure 1. Gas molecules near the corona discharge region become ionized when a high intensity electric field is applied between a high tip curvature corona electrode and a low tip curvature collector electrode. In the case of a wire or rod electrode, the diameter of the electrode is equivalent to the tip curvature of a needle electrode.

The ionized gas molecules travel towards the collector electrode, colliding with neutral air molecules. During these collisions, momentum is transferred from the ionized gas into the neutral air molecules, resulting in bulk gas movement towards the collector electrode. The operating voltage range for corona discharge lies between the corona onset and air gap breakdown voltage [7]. Corona induced airflow is possible with both a positive and negative voltage. However, higher stream velocity can be achieved by using positive polarity [8]. The first documentation of corona wind came as early as the 1700's [9], and has been investigated by numerous researchers, including Newton, Faraday, and Maxwell. Some of the first rigorous fundamental studies were conducted by Stuetzer [10], who investigated ion conduction in both liquids and gases, and Robinson [11] who investigated corona wind pressure, electric parameters and efficiency in ambient air conditions. More recent studies include such applications as filtration [12], air sterilization, and dehumidification [13].

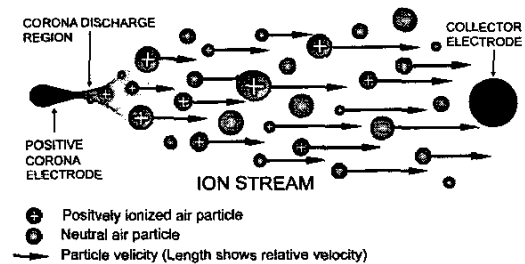


**Figure 1.** Ion stream of a DC electrostatic air pump, where a high voltage is applied between the corona and collector electrodes.

### Simulation Setup and Procedure

Finite element simulations for a sharp-edge-to-parallel-plane corona pump geometry with an applied distributed collector were performed. The electrostatic vector fields were calculated within the simulated pump. Electric field values were used to calculate relative efficiency between various collector voltage distributions based on the figure of merit calculations.

### Pump design

Figure 2 shows a sharp-edge-to-parallel-plane ionic wind pump geometry. The sharp-edge-to-parallel-plane configuration was chosen for this study due to several advantages over the classic point-to-plane and wire-to-rod geometries. This geometry allows the use of thin collector electrodes and substantially decreases air resistance. The sharp-edge-to-parallel-plane assembly utilizes a razor-like corona electrode, allowing for electrode wear without significant tip curvature degradation or structural fatigue. Corona electrode surface erosion from a wire-to-rod configuration is shown in Figure 3. Corona electrode erosion can lead to nonuniform corona discharge and eventual device failure. The use of a sharp-edge corona electrode minimizes the impact of erosion, extending device life. The sharp-edge-to-parallel-plane regime decreases pump air resistance by moving the collector electrode from the main airflow path as in Figure 1, to the sides of the corona electrode. With the collector electrodes positioned at the sides of the airflow, it is possible to control the electric field as a function of distance along the collector electrode by applying a distributed voltage along the collector surface. Control over the electric field geometry makes it possible to control the distribution of the of the columbic forces acting on the ions within the pump, making it possible to control airflow profiles.

### Simulation Parameters

Simulations for a sharp-edge-to-parallel-plane geometry were conducted with Ansoft Maxwell EM 2D electrostatic field solver. The simulation space was broken down into five regions as follows: the surrounding air environment, an insulating support structure, a conductive collector electrode on the inner wall of the insulating support structure, the region between the two collector electrodes where a space charge was defined for this simulation, and, finally, a corona electrode, modeled as a perfect conductor.

A positive voltage of 10 kV was applied to the corona tip. The voltage applied to the curved collector electrode was modeled as a linear function from 0 volts at the top to a higher voltage from (0.1 kV to 5 kV) at the bottom. Space charge was included in the simulation to account for the electric field generated from the ion stream passing between corona and collector electrodes. When simulating with a space charge, a charge density of  $10^{-4} \text{ C/m}^3$  placed at the corona tip was decreasing linearly by  $10^{-5} \text{ C/m}^3$  per cm in the direction of airflow within the collector channel. This space charge value was adapted from earlier corona pump space charge models [3], which

approximate the values measured indirectly in prior experimental studies. A coupled field simulation that takes into account fluid dynamics and space charge generation would have been a more complete model of this system, but is viewed by the authors as unnecessarily complex for the purpose of this study.

The electric field distribution was calculated in the entire simulation space. The internal functions of the Maxwell software do not easily allow for the desired calculations, therefore the data was exported by macros and post-processed with Matlab. For this purpose, the pump device space was divided into 45 linear horizontal segments stacked in the vertical direction. Each of the segments can be seen as an array of horizontal lines within the force vector plots in Figure 5 through Figure 8. Along each segment, a horizontal line orthogonal to the direction of airflow is drawn. Along each line, the x and y electric field vector magnitude was extracted from the numerical simulation results to be used in figure of merit pump efficiency comparison calculations.

### Figure of merit calculations

The figure of merit (FoM) calculations act as a metric to quantitatively compare efficiency between different pump designs and different voltage distributions for each design. Columbic forces induced on charges by the electric field generate airflow. The force vector applied to a charge within the pump can be separated into two components, the first component in the direction of intended airflow, x, and the second orthogonal to intended airflow, y. The greater the ratio of the x to y direction components, the greater the predicted efficiency is of the system.

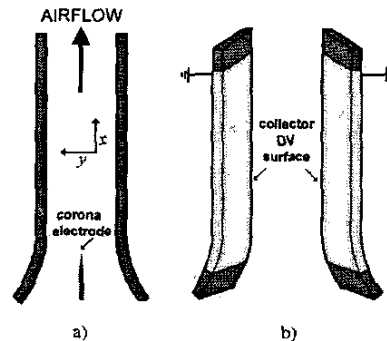


Figure 2. (a) side view of the sharp-edge-to-parallel-plane corona pump structure; (b) a continuous voltage gradient is generated along collector distributed voltage (DV) surface.

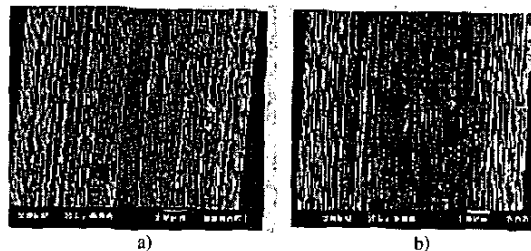


Figure 3. SEM photo of corona electrode surface erosion in the wire-to-rod configuration: a) wire surface before use, b) wire surface after several hours of intensive corona discharge.

The procedure for calculating the FoM is as follows. Electric field magnitudes  $E_x$  and  $E_y$  are multiplied by the unit charge  $\rho$ , converting them to coulombic force values,  $f_x$  and  $f_y$ . The  $f_x$  and  $f_y$  values are integrated along all 45 horizontal lines giving  $F_x$  and  $F_y$ . A ratio is taken of the  $F_x$  and  $F_y$  scalars giving the FoM value  $f_m$  shown below (1).

$$f_m = \frac{F_x}{F_y} = \frac{\iint_A \rho \cdot |E_x| dx dy}{\iint_A \rho \cdot |E_y| dx dy} \quad (1)$$

The double integral in (1) is taken over the area enclosed by the collector electrodes in the cross-section simulation space.

### Simulation Results

Corona pump optimization using a distributed voltage along the collector electrode was found to be possible. A positive correlation between the calculated FoM and the magnitude of the voltage distributed along the length of the collector electrode is shown in Figure 4. As the voltage distributed over the collector increases from 0 V (Figure 5 and Figure 7) to 5 kV (Figure 6 and Figure 8), the equipotential voltage lines within the corona air pump channel become more horizontal, and the electric field, shown as arrows, becomes better aligned with the pump flow. All equipotential voltage lines are separated by 416 V, which is calculated by dividing the total voltage drop between the corona and collector electrodes by 24, the number of equipotential lines for each plot. A collector distributed voltage increase from 0 V to 5 kV resulted in a FoM increase of 74.3%.

The effect of space charge on the electric field can be seen best by comparing equipotential lines within the pump channel in Figure 6 and Figure 8. The equipotential field lines within the pump channel are nearly parallel to each other and orthogonal to pump flow in Figure 6, where no space charge is present. As space charge is introduced, Figure 8, it changes the electric field distribution, resulting in a more curved equipotential line. The space charge is composed of the ions within the pump. Since all the floating charges outside the corona discharge region are of the same polarity as the corona electrode, they reduce the electric field generated by the corona and collector electrodes. This effect is most pronounced around the corona electrode and in the region of ion flow.

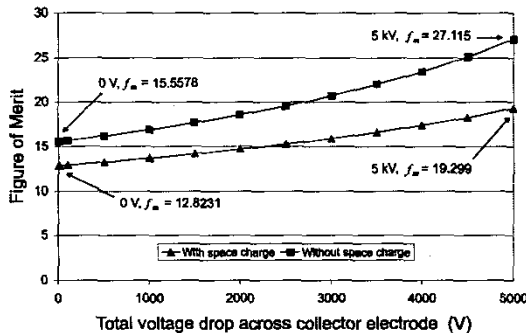


Figure 4. Relationship between the FoM and total voltage drop of distributed collector voltage, with and without space charge.

The reduction of the electric field in these regions results in a smoothing or decreasing of the electric field around the corona tip and along the center of the channel. The resulting decrease in FoM caused by including space charge in the simulations is displayed in Figure 4, ranging from 17% to 28% for the lowest and highest distributed voltage, respectively.

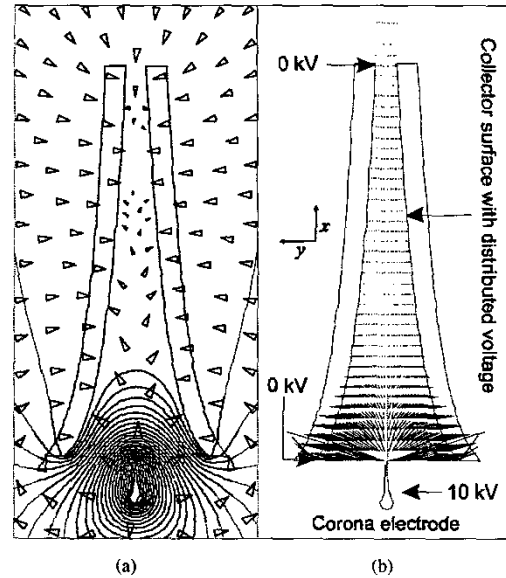


Figure 5. Simulation plots for a grounded collector electrode without an applied space charge: (a) equipotential lines and electric field shown as arrows scaled logarithmically with the field magnitude; (b) calculated coulombic force vectors within pump channel used to compute the FoM value, 15.5778 for this simulation.

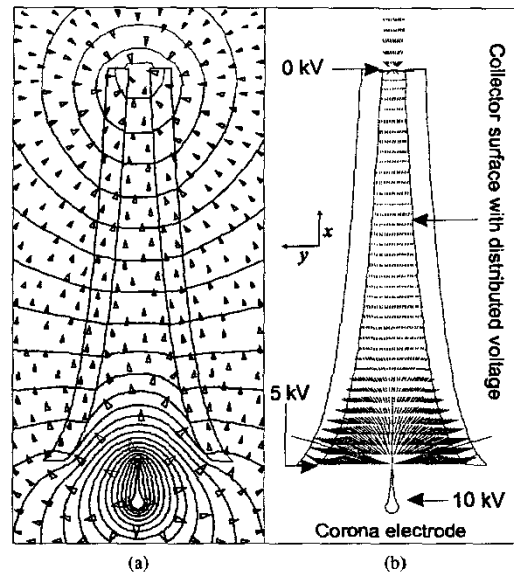
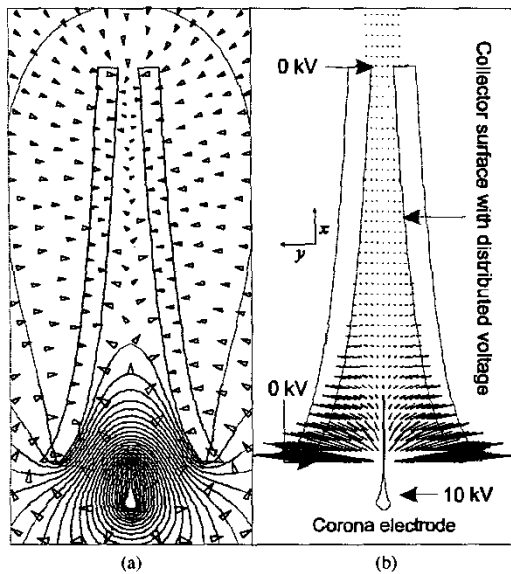
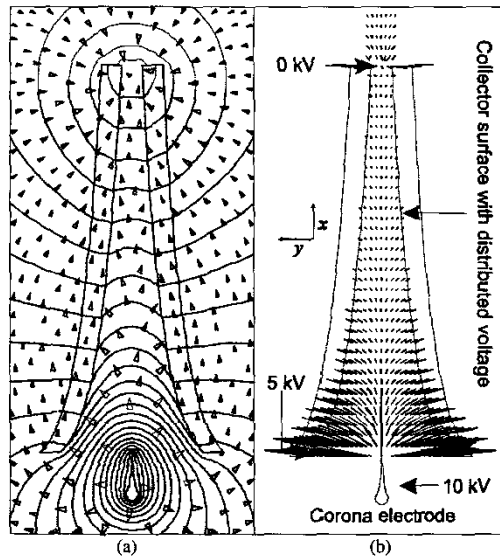


Figure 6. Simulation plots for a collector electrode distributed voltage of 5 kV without an applied space charge: (a) equipotential lines and electric field shown as arrows scaled logarithmically with the field magnitude; (b) calculated coulombic force vectors within pump channel used to compute the FoM value, 27.1154 for this simulation.



**Figure 7.** Simulation plots for a grounded collector electrode with an applied space charge. (a) : (a) equipotential lines and electric field shown as arrows scaled logarithmically with the field magnitude; (b) calculated columbic force vectors within pump channel used to compute the FoM value, 12.8231 for this simulation.



**Figure 8.** Simulation plots for a collector electrode distributed voltage of 5 kV with an applied space charge: (a) equipotential lines and electric field shown as arrows scaled logarithmically with the field magnitude; (b) calculated columbic force vectors within pump channel used to compute the FoM value, 19.299 for this simulation.

### Conclusions and Future Work

This paper presented an optimization study for ionic wind electrostatic pumps. The concept of a figure of merit (FoM) to compare quantitatively the efficiency of pump designs and voltage distributions was proposed. The FoM was computed for several designs. Device optimization through the application of a distributed collector voltage was shown to be possible. The effect of space charge on device performance was

illustrated. Future work will investigate the distributed voltage optimization strategy with more complex and dynamically varying voltages in order to improve performance of electrostatic air pumps, dehumidifiers, and other corona based devices. FoM efficiency calculations should be expanded to other corona based devices and coupled with simulations that take into account actual space charge distributions and fluid dynamics.

### Acknowledgments

Financial support has been provided by the Army Research Office grant # DACA42-02-0023 awarded to Kronos Air Technologies, Inc. Additional student support was provided by the Grainger Foundation and the American Public Power Association Demonstration of Energy-Efficient Developments (APPA DEED) Program with the assistance of Seattle City Light. Undergraduate research scholarships were funded by the University of Washington Mary Gates Research Training Grant, the Washington NASA Space Grant Consortium, and the Electrical Energy Industrial Consortium. The donation of software by Ansoft Corp. is greatly appreciated.

### References

- [1] J. Mathew and F. C. Lai, "Enhanced Heat Transfer in a Horizontal Channel With Double Electrodes," *IEEE Industry Applications Conference*, vol. 2, 1995, pp. 1472-1479.
- [2] A. Rashkovan, E. Sher, and H. Kalman, "Experimental Optimization of an Electric Blower by Corona Wind," *Applied Thermal Engineering*, vol. 22, no. 14, pp. 1587-1599, Oct. 2002.
- [3] G. M. Colver and S. El-Khabiry, "Modeling of DC Corona Discharge Along an Electrically Conductive Flat Plate With Gas Flow," *IEEE Transactions on Industry Applications*, vol. 35, no. 2, pp. 387-394, Mar. 1999.
- [4] D. Schilitz, S. Garimella, and T. Fisher, "Numerical Simulation of Microscale Ion Driven Air Flow," *ASME IMECE*, Washington DC, 2003.
- [5] F. Yang, "Corona-driven air propulsion for cooling of microelectronics," Masters Thesis, Department of Electrical Engineering, University of Washington, 2002.
- [6] F. Yang, N. E. Jewell-Larsen, D. L. Brown, D. A. Parker, K. A. Pendergrass, I. A. Krichtafovich, and A. V. Mamishev, "Corona Driven Air Propulsion for Cooling of Electronics," *International Symposium on High Voltage Engineering*, Delft, Netherlands, 2003.
- [7] F. W. Peek, *Dielectric Phenomena in High Voltage Engineering*, New York:McGraw-Hill, 1929.
- [8] E. Sher, "Extinction of Pool Flames by Means of a DC Electric Field," *Combustion and Flame*, 1994.
- [9] F. Hauksbee, *Physico-Mechanical Experiments on Various Subjects*, London, England, 1709, pp. 46-47.
- [10] O. M. Stuetzer, "Ion Drag Pressure Generation," *Journal of Applied Physics*, vol. 30, no. 7, pp. 984-994, July 1959.
- [11] M. Robinson, "Movement of Air in the Electronic Wind of Corona Discharge," *AIEE Transactions*, vol. 80, pp. 143-150, May 1961.
- [12] K. J. Mclean, "Electrostatic Precipitators," *IEE Proceedings on Science Measurement and Technology*, vol. 135, no. 6, pp. 347-361, July 1988.
- [13] M. Jyumonji and H. Uchiyama, "Field Experiment on the Abatement of Stock-Raising Odors by an Electrostatic Fog-Liquefier," *Journal of Electrostatics*, vol. 40-1, pp. 645-650, June 1997.